JOURNAL OF MATERIALS SCIENCE 12 (1977) 2269–2273

Influence of elastic and thermal mismatch on the local crack-driving force in brittle composites

A. K. KHAUND, V. D. KRSTIC, P. S. NICHOLSON
Department of Metallurgy and Materials Science, McMaster University, Hamilton, Ontario, Canada

An expression is derived for the change of local K_I value of a crackfront near circular and spherical inclusions with elastic moduli and thermal expansion coefficient different from those of the matrix. The derivation is based on the concept of an "image stress" which is imposed on the crack, to illustrate the interaction between elastic and thermal stress concentrations developed around inclusions in a composite material and the crack-tip stress field.

1. Introduction

It is known [1, 2] that second phase inclusions (or pores) with different elastic moduli and thermal expansion coefficients give rise to local stress concentrations in a composite material. Using the complex variable approach and the elastic solutions given by Muskhelishvili [3], Tamate [4] and Tirosh and Tetelman [5] have shown that there occurs a change in stress intensity factor for a crack approaching a cylindrical inclusion.

The problem treated herein concerns the interaction between the crack-tip stress field and the stress concentrations developed around circular and spherical inclusions (or pores) with different elastic and thermal expansion coefficients. The solutions for the elastic stress concentrations around circular and spherical inclusions (or pores) due to an applied uniaxial tension are taken from Goodier's [1] treatment. An approach is adopted which gives a simple analytical solution for the change of local crack driving force caused by the elastic and thermal stresses around inclusions (or pores). The results are discussed in the light of available literature.

2. Analysis

When a load is applied to propagate a crack (Mode I, i.e. where a tensile load is applied normal to the crack surfaces) in a composite, a stress field is also generated around the inclusions due to elastic mismatch, For example, the two-dimensional form of iso-stress contours for the tangential component ($\sigma_{\theta\theta}$) around an Al_2O_3 sphere and a pore in a glass matrix are shown in Fig. 1 (based on Goodier's [1] treatment). Differences of thermal expansion coefficient give rise to hydrostatic stresses around inclusions [2] when composite materials are cooled from fabrication temperature. An estimate of the change of local K_I values for a crack in a composite due to these stress fields can be made using the concept of an "image stress" on the crack front due to the inclusion it is approaching.

Consider a crack moving on an infinite plane coincident with the equatorial plane of an inclusion (Fig. 2). A biaxial stress condition exists along this plane. If σ_a is the applied stress in a body containing no inhomogeneities, introduction of a second phase of different elastic properties will change the stress conditions of the body, i.e.

$$\sigma_{new} = (\sigma_i)_{\text{due to } \sigma_a} - \sigma_a \tag{1}$$

where σ_i is the stress concentration due to the presence of the inclusions in the applied stress field (σ_a) in the absence of a crack. When a crack-front is very near the inclusion, σ_i will mostly result from the σ_{yy} component of the crack field and the effect of σ_a will be negligible in this case. Hence, under this condition

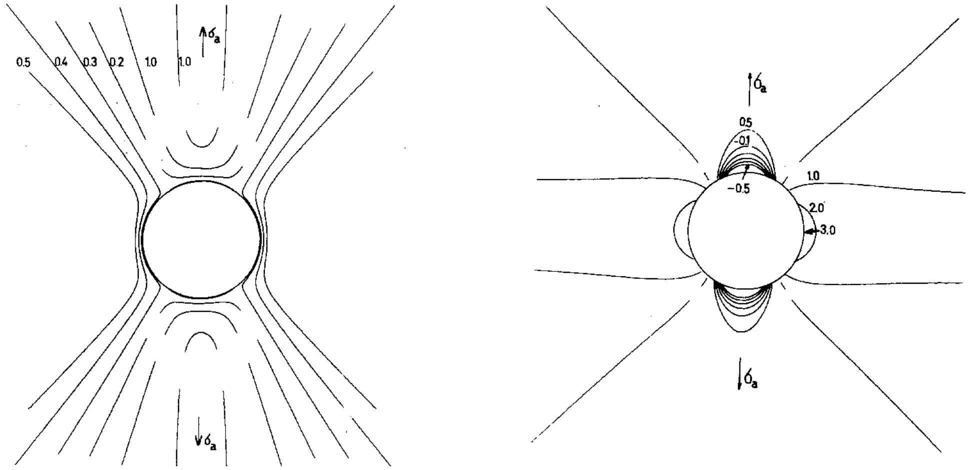

Figure 1 $\sigma_{\theta\theta}/\sigma_a$ for (a) Al_2O_3 in glass and (b) pore in glass. (The digits represent values of σ/σ_a).

$$\sigma_{new} = (\sigma_i)_{\text{due to }\sigma_{yy}} - (\sigma)_{yy} \tag{2}$$

Now the σ_i along the equatorial plane of a circular and spherical inclusion due to an applied stress (in this case the biaxial crackfront stress, where $\sigma_{yy} = \sigma_{xx}$ along the $\theta' = 0°$ direction) can be found by considering Goodier's solution [1] for the tangential component of the stress field around a circular inclusion;

$$\sigma_{\theta\theta} = 2\sigma_a\left[A\left(\frac{r}{s}\right)^2 - 3B\left(\frac{r}{s}\right)^4 \cos 2\theta\right] + \frac{\sigma_a}{2}(1-\cos 2\theta) \tag{3}$$

and around a spherical inclusion

$$\sigma_{\theta\theta} = \frac{\sigma_a}{2}\left[-\frac{A'r^3}{s^3} - \frac{2\nu_m}{1-2\nu_m}\frac{C'r^3}{s^3} - \frac{3B'r^5}{s^5} + \left(3\frac{C'r^3}{s^3} - 21\frac{B'r^5}{s^5}\right)\cos 2\theta\right] + \frac{\sigma_a}{2}(1-\cos 2\theta) \tag{4}$$

In Equations 3 and 4, r is the radius of the inclusion, s is the distance from the centre of the inclusion (see Fig. 2) and A, B, A', B' and C' are constants whose values depend on the elastic mismatch:

$$A = \frac{(1-2\nu_i)G_m}{4((1-2\nu_i)G_m + G_i)}$$

$$B = \frac{G_m - G_i}{4(G_m + (3-4\nu_m)G_i)}$$

$$A' = \frac{G_m - G_i}{2(7-5\nu_m)G_m + (8-10\nu_m)G_i} \times \frac{(1-2\nu_i)(6-5\nu_m)2G_m + (3+19\nu_i - 20\nu_m\nu_i)G_i}{(1-2\nu_i)2G_m + (1+\nu_i)G_i} + \frac{[(1-\nu_m)(1+\nu_i)/(1+\nu_m) - \nu_i]G_i - (1-2\nu_i)G_m}{(1-2\nu_i)2G_m + (1+\nu_i)G_i}$$

$$B' = \frac{G_m - G_i}{2(7-5\nu_m)G_m + (8-10\nu_m)G_i}$$

$$C' = \frac{5(1-2\nu_m)(G_m - G_i)}{2(7-5\nu_m)G_m + (8-10\nu_m)G_i}$$

where G_m and G_i are the rigidity moduli for the matrix and inclusion, respectively, and ν_m and ν_i are the Poisson's ratios for the matrix and inclusion.

Now for $\theta = \theta + \frac{\pi}{2}$, from Equation 3, it follows that, for circular inclusion,

$$(\sigma_{\theta\theta})_{\theta=\theta+\frac{\pi}{2}} = \frac{\sigma_a}{2}(1+\cos 2\theta) + 2\sigma_a\left[A\left(\frac{r}{s}\right)^2 + 3B\left(\frac{r}{s}\right)^4\cos 2\theta\right] \tag{5}$$

Hence in any direction, the biaxial tangential component of stress due to the inclusion is (by addition of Equations 3 and 5

$$(\sigma_{\theta\theta})_{biaxial} = \sigma_a + 4A\sigma_a\left(\frac{r}{s}\right)^2 = (\sigma_i)_{\text{due to }\sigma_a}. \tag{6}$$

When the crack-front is very close to the inclusion and is running in the $\theta' = 0°$ direction (Fig. 2), Equation 6 modifies (as $\sigma_{yy} \gg \sigma_a$) to

$$(\sigma_{\theta\theta})_{\text{biaxial}} = (\sigma_{yy})_{\theta'=0°} + 4[(\sigma_{yy})_{\theta'=0°}]A\left(\frac{r}{s}\right)^2$$
$$= (\sigma_i)_{\text{due to } \sigma_{yy}} \tag{7}$$

Hence, the "new stress" acting along the crack-front when it is very near the inclusion will be (from Equations 2 and 7)

$$\sigma_{\text{new}} = (\sigma_{\theta\theta})_{\text{biaxial}} - (\sigma_{yy})_{\theta'=0}$$
$$= 4A\left(\frac{r}{s}\right)^2 [(\sigma_{yy})_{\theta'=0}]$$
$$= 4A\left(\frac{r}{s}\right)^2 \frac{K_I}{\sqrt{2\pi t}} \tag{8}$$

where t is the distance of the crack-front from the centre of the inclusion and K_I is the stress intensity factor (Mode I) at the crack tip in the absence of the inclusion. This σ_{new} will change the value of the crack intensity factor K_1 of the crack-front by "ΔK", restricted by the following boundary condition for the crack shown in Fig. 2.

$$\Delta K - \int_{s=\infty}^{s=t} \sigma_{\text{image}} \sqrt{\left(\frac{2}{\pi(s-t)}\right)} \, ds = 0 \tag{9}$$

where σ_{image} is equal to σ_{new} as given in Equation 8 but is acting in the opposite direction so as to satisfy the condition given in Equation 9. Hence, from Equation 9,

$$\Delta K = \sigma_{\text{new}} \int_{s=\infty}^{s=t} \sqrt{\left(\frac{2}{\pi(s-t)}\right)} \, ds$$
$$= \frac{4Ar^2 K_I}{\pi\sqrt{(t)}} \int_{s=\infty}^{s=t} \frac{ds}{s^2(s-t)^{1/2}}$$
$$= -\frac{2Ar^2}{t^2} K_I. \tag{10}$$

Therefore, for circular inclusion

$$(K_{\text{new}})_{\text{elastic mismatch}} = K_I - \Delta K = K_I\left(1 + \frac{2Ar^2}{t^2}\right) \tag{11}$$

Similarly for a spherical inclusion, using Equation 4 for $\sigma_{\theta\theta}$ and going through the same procedures from Equations 5 to 8, we have,

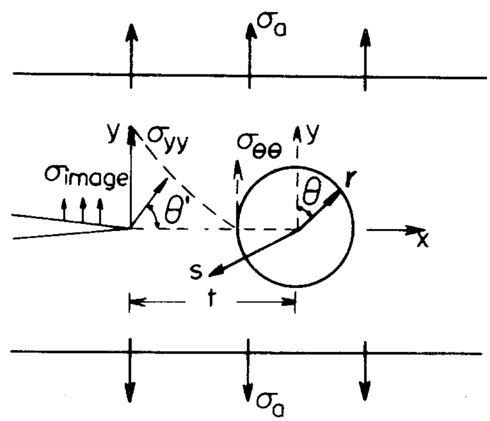

Figure 2 The interaction between an inclusion and a crack in the matrix in the near vicinity of the inclusion.

$$(\sigma_{\text{new}})_{\text{spherical}} = \frac{K_I}{\sqrt{(2)\pi t}} \left(-\frac{A'r^3}{s^3} - \frac{2\nu_m}{1-2\nu_m}\frac{C'r^3}{s^3} - \frac{3B'r^5}{s^5}\right). \tag{12}$$

When the crack-front approaches the spherical inclusion, the condition given in Equation 9 must be satisfied, hence (as in Equation 10),

$$\Delta K = (\sigma_{\text{new}})_{\text{spherical}} \int_{s=\infty}^{s=t} \sqrt{\left(\frac{2}{\pi(s-t)}\right)} ds$$
$$= -\frac{A'r^3 K_I}{\pi\sqrt{(t)}} \int_{s=\infty}^{s=t} \frac{ds}{s^3(s-t)^{1/2}}$$
$$- \frac{2\nu_m C' r^3 K_I}{(1-2\nu_m)\pi\sqrt{(t)}} \int_{s=\infty}^{s=t} \frac{ds}{s^3(s-t)^{1/2}}$$
$$- \frac{3B'r^5 K_I}{\pi\sqrt{(t)}} \int_{s=\infty}^{s=t} \frac{ds}{s^5(s-t)^{1/2}}$$
$$= \left(0.39A'\frac{r^3}{t^3} + \frac{0.78\nu_m C'}{1-2\nu_m}\frac{r^3}{t^3} + 0.820B'\frac{r^5}{t^5}\right)K_I.$$

Hence, for spherical inclusion,

$$(K_{\text{new}})_{\text{elastic mismatch}} = K_I - \Delta K =$$
$$K_I\left[1 - 0.39A'\frac{r^3}{t^3} - \frac{0.78\nu_m C'}{(1-2\nu_m)}\frac{r^3}{t^3} - 0.820B'\frac{r^5}{r^5}\right] \tag{13}$$

The effect of thermal residual stress on the K_I value can be estimated using the tangential component of the residual stress given by [2]

$$\sigma_{\theta\theta} = \frac{1}{2}\beta\left(\frac{r}{s}\right)^3, \tag{14}$$

where

$$\beta = \frac{\Delta\alpha\Delta T}{\left(\dfrac{1+\nu_m}{2E_m}\right)+\left(\dfrac{1-\nu_i}{2E_i}\right)}$$

E_m, E_i, ν_m, ν_i are the Young's moduli and Poisson's ratio for the matrix and inclusion respectively, $\Delta\alpha$ is the difference in thermal expansion coefficients between matrix and inclusion, and ΔT is the temperature difference. Hence, as in the case of the "elastic mismatch".

$$\Delta K = \sigma_{\text{new}} \int_{s=\infty}^{s=t} \sqrt{\left(\frac{2}{\pi(s-t)}\right)} \mathrm{d}s$$

$$= \frac{\beta r^3}{\sqrt{(2\pi)}} \int_{s=\infty}^{s=t} \frac{\mathrm{d}s}{s^3(s-t)^{1/2}} = -0.470\beta r^3/t^{5/2}$$

Hence,

$$(K_{\text{new}})_{\text{thermal mismatch}} = K_I + 0.470\beta r^3/t^{5/2}$$

Equations 13 and 15 are valid for a crack approaching a single inclusion. If the crack-front meets a linear array of similar obstacles with an average inter-obstacle spacing d, then

$$(\Delta K)_{\text{average}} = \frac{2}{d}\int_{t=d/2}^{r} (\Delta K)\mathrm{d}t. \tag{16}$$

3. Discussion

From the foregoing analysis (Equation 13), it is evident that the nature of the influence of an inclusion and a pore on the crack-driving force K_I (Mode I) of an approaching crack-front is clearly different and is characterized by the value of elastic mismatch coefficients A', B' and C' (given in Equation 4). If the values of A', B' and C' are such that $K_{\text{new}} < K$, then the velocity of the crack-front would decrease as it approaches the inclusion; on the other hand if the value of A', B' and C' are such that $K_{\text{new}} > K$, then the velocity of the crack-front will increase as it approaches the inhomogeneity. For example, in glass–Al_2O_3 composite $A' = 0.458$, $B' = -0.166$ and $C' = -0.50$, so $K_{\text{new}} < K$ in this case, and the velocity of the crack-front should locally decrease as it approaches a spherical alumina inclusion in a glass matrix. In fact the

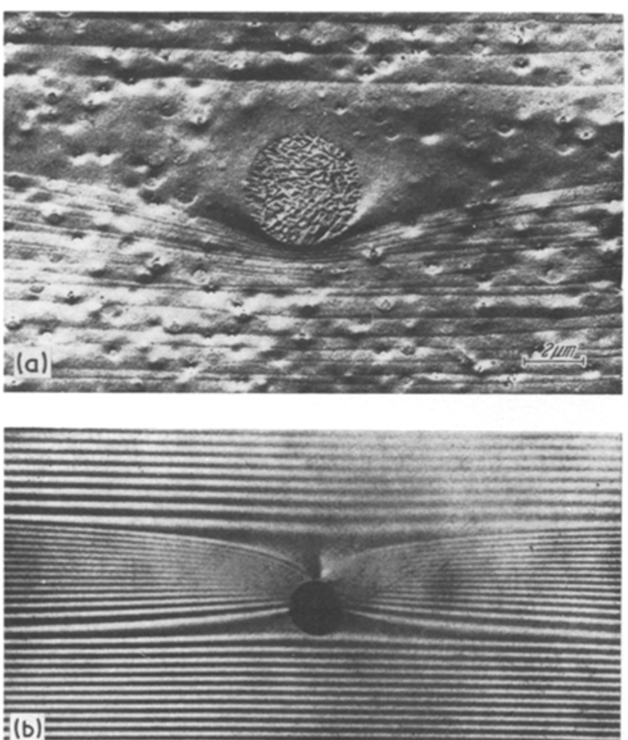

Figure 3 (a) Crack-front shapes in a glass matrix near an inclusion [6]. (b) Crack-front shapes in a glass matrix near a pore [7]. (Direction of crack propagation is from the bottom to the top.)

velocity will be decreased for a spherical inclusion for which $G_i > G_m$, as the coefficient A' is always positive in these case. For a pore $G_i = 0$ ($< G_m$), so that $K_{new} > K$ in this case (from Equation 13), and an approaching crack-front will be locally accelerated. Two such distinct behavioural changes of crack-front shape were experimentally observed for inclusion/glass and capillary pore/glass systems shown in the ultransonically modulated fracture surface photographs, Figs. 3a and b [6, 7].

In the photographs the distance between the ripples gives a measure of the velocity of the crack-front. The nature of the influcence of the inclusion with $G_i > G_m$ and the pore with $G_i = 0$ ($< G_m$) on the crack-front, qualitatively agrees with the result of Tirosh and Tetelman [4]. However, the changes of K_I value for a crack near an inclusion (or pore) are usually small; for example ~10% for Al_2O_3 inclusion in glass and ~25% for a pore in glass, when the crack-front is very close to the inclusion or to the pore. Hence, the local deceleration (or acceleration) of a crack-front near an inclusion ($G_i > G_m$) or pore ($G_i = 0 < G_m$) will be small and hence its contribution to the large increase in toughening observed in composite materials [8] may also be small. Changes in the crack-driving force due to thermal mismatch are even smaller compared to the elastic mismatch contribution. In the thermal case, the change in crack-front velocity (and hence shape) depends on the thermal mismatch coefficient β (see Equation 12). In the case of glass–Al_2O_3 composite, $\beta \simeq 3.4 \times 10^8$ dynes cm^{-2} (when $\alpha_i > \alpha_m$) giving a resultant change in K_I values by less than 2% for $K_I = 60\% K_{IC}$ (the thermal mismatch effect may be significant; however, if the localized residual stress cracks the particle/matrix interface or gives rise to adjacent microflaws). Such small effect of elastic and thermal mismatches on the K_I values for an approaching crack-front justify, to a first approximation, the assumptions made in several models [8, 9] (put forward to explain the observed toughness in composite materials) that the crack-front in uninfluenced by elastic and thermal mismatch. However, the presence of elastic stress concentration (σ_{rr}) at the poles of the inclusion may alter the direction of propagation of a crack as it approaches the inclusion.

The present analysis illustrates that, depending on the nature of elastic mismatch (i.e. on the value of coefficient A', B' and C') between matrix and inclusion (or pore), the crack-front will respond differently. The effect of thermal mismatch on local K_I values for an approaching crack-front is negligibly small.

Acknowledgments
The authors express their appreciation to Dr R. G. Hoagland from Batelle Memorial Institute, Columbus, Ohio for suggesting the use of the image stress concept to solve the problem. The authors would also like to thank Mr D. J. Green for pointing out a computational error in the manuscript.

References
1. J. N. GOODIER, *J. Appl. Mech.* **1** (1933) 39.
2. J. SELSING, *J. Amer. Ceram. Soc.* **44** (1967) 44.
3. N. I. MUSKHELISHVILI, "Some Basic Problems of the Mathematical Theory of Elasticity" (Noordhoff, Leyden, 1975).
4. O. TAMATE, *Int. J. Frac. Mech.* **4** (1968) 257.
5. J. TIROSH and A. S. TETELMAN, *ibid* **12** (1976) 187.
6. F. KIRKHOFF, "Bruchovogange in Glassen", (Verlag der Deutch Glastech Ges., Frankfurt, 1970).
7. F. KIRKHOFF and E. SOMMER, "Handbuch der Mikroskopie in der Technik", (Springer, West Germany, 1960).
8. F. F. LANGE, *J. Amer. Ceram. Soc.* **54** (1971) 614.
9. A. G. EVANS, *Phil. Mag.* **7** (1972) 1327.

Received 14 December 1976 and accepted 11 March 1977.